Dissociation–equilibrium constant and bound conformation for weak antibiotic binding interaction with different bacterial ribosomes †

Laurent Verdier,[a] Josyane Gharbi-Benarous,[a,b] Gildas Bertho,[a] Nathalie Evrard-Todeschi,[a] Pascale Mauvais[c] and Jean-Pierre Girault *[a]

[a] *Université René Descartes-Paris V, Laboratoire de Chimie et Biochimie Pharmacologiques et Toxicologiques (UMR 8601 CNRS), 45 rue des Saint-Pères, 75270 Paris Cedex 06, France*
[b] *Université Denis Diderot-Paris VII, UFR Chimie, 2 Place Jussieu, F-75251 Paris Cedex 05, France*
[c] *Hoechst Marion Roussel, 102 route de Noisy, 93235 Romainville Cedex, France*

Received (in Cambridge, UK) 21st September 2000, Accepted 20th October 2000
First published as an Advance Article on the web 16th November 2000

This paper characterises low-affinity antibiotic binding interactions by the T_2 (CPMG) method. Three different compounds, a ketolide 'telithromycin' (HMR 3647), a macrolide 'roxithromycin' and a lincosamide 'clindamycin' belonging to the macrolide–lincosamide–streptogramin B (MLS_B) class of antimicrobial agents were examined against *Escherichia coli*, *Streptococcus pneumoniae* and *Staphylococcus aureus* strains. The Carr–Purcell–Meiboom–Gill spin-echo decay rate allows determination of the ^{1}H-NMR transverse relaxation (T_2). T_2 (CPMG) measurements represent a sensitive method and they can be used to characterise equilibrium binding of low-affinity antibiotics to bacterial ribosomes. This analysis revealed weak binding of telithromycin, roxithromycin and clindamycin with respectively, $K_D = 1.2 \times 10^{-3}$, 1.3×10^{-3} and 1.3×10^{-2} to *E. coli*, 3.4×10^{-4}, 3.6×10^{-3} and 1.4×10^{-3} to *S. pneumoniae* and 3.1×10^{-3}, 7.9×10^{-3} and 2.9×10^{-3} to *S. aureus*. Additionally, this paper demonstrates by a study using 2D transferred nuclear Overhauser effect spectroscopy (TRNOESY), that the three MLS_B antibiotics exist in these ribosome binding sites in certain conformations. Analysis of the TRNOE experiments resulted in a set of constraints for all proton pairs. These constraints were used in structure determination procedures based on molecular modelling to obtain the conformation of the antibiotic in its bound state. This study allowed us to compare the bound structure at the bacterial ribosomes for the active ketolide and MLS_B antibiotics and to bring to the fore an interesting relationship between the conformation of the antibiotic when interacting and its activity. The weak interaction responses to *S. pneumoniae* and *S. aureus* strains require a '**B**' conformation which is especially favoured for the ketolide telithromycin.

Introduction

MLS_B (Macrolide, Lincosamide and Streptogramin B) antibiotics inhibit protein biosynthesis in the elongation step by binding to the 50S bacterial ribosomes.[1] There appear to be two stages in this binding: a weak interaction that can be detected by NMR spectroscopy,[2] and a stronger interaction ($K_D = 10^{-7}$–10^{-9} M)[3–5] detected by equilibrium dialysis and related methods. The weak interactions observed by NMR are in agreement with a hypothesis of two distinct binding levels, with a low-affinity pre-inhibition binding level and the tight inhibition binding one responsible for protein biosynthesis inhibition.[6] This weak binding observed by TRNOE experiments could be involved in the first step of recognition and selection of antibiotics by the ribosomal machinery. Compounds which are not able to take part in a weak binding interaction with bacterial ribosomes do not exert antibiotic activity,[2] which was also observed by Barber *et al.*[6,7] Thus, the weak binding site seems to be a necessary step for the strong interaction.

In this study, we have utilised ^{1}H-NMR spectroscopy to directly observe and characterise MLS_B antibiotic weak binding to bacterial ribosomes. The NMR analysis takes advantage of the fact that antibiotic molecules rapidly exchange between ribosome-bound and aqueous free states. The rapid exchange results in a single observable antibiotic NMR signal that contains information concerning both the bound and free states. There are three main approaches for the NMR measurement of the equilibrium dissociation constant K_D: (i) binding-induced line broadening ($\Delta\nu$) in the NMR spectra, (ii) $T_1\rho$ (the decay rate of spin-locked magnetisation in the rotating frame), (iii) T_2 (CPMG) methods.[8,9] Particular emphasis is given to an analysis of the spin–spin (T_2) behaviour[10] of the exchanging system in order to determine the ligand equilibrium binding constant (K_D).

This paper reports direct measurements of the dissociation equilibrium constants (K_D) for the antibiotic–ribosome complex by the T_2 (CPMG) method for low affinity antibiotic binding interactions with bacterial ribosomes. The study started with the antibiotic *E. coli* ribosome weak interactions and then was extended to erythromycin-sensitive and -resistant strains, constitutive (EryRc) phenotypes of *Streptococcus pneumoniae* and *Staphylococcus aureus*. Three different compounds belonging to the MLS_B class of antimicrobial agents were tested, a ketolide 'telithromycin' (HMR 3647) (**1**), a macrolide 'roxithromycin' (**2**) and a lincosamide 'clindamycin' (**3**) (Fig. 1).

† Tables S1–S3 for **1**–**3**, respectively, containing data for the TRNOE spectra recorded in the presence of *E. coli*, *S. pneumoniae* and *S. aureus* ribosomes; Fig. S1 for **1** and Fig. S2 for **2** and **3** of plots [eqn. (5)] with the different ribosomes; Fig. S3 of the ^{1}H-NMR line-broadening for **1**–**3** with *E. coli* ribosome are available as supplementary data. For direct electronic access see http://www.rsc.org/suppdata/p2/b0/b007666j/

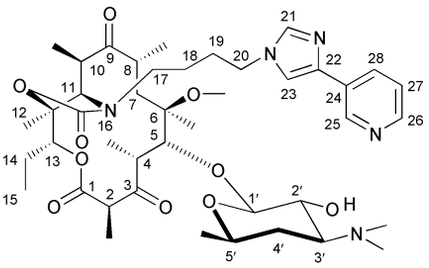

telithromycin (**1**)

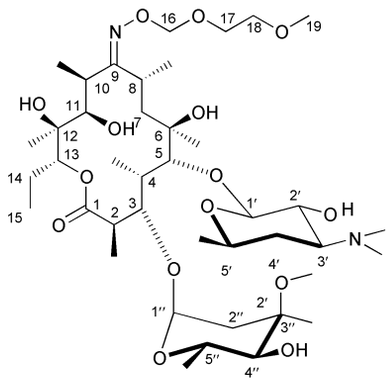

roxithromycin (**2**)

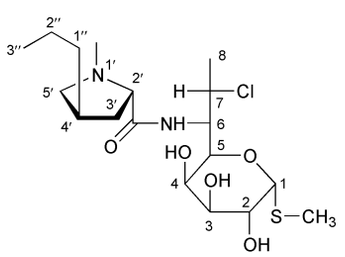

clindamycin (**3**)

Fig. 1 Structures of ketolide, telithromycin (**1**); macrolide, roxithromycin (**2**) and lincosamide, clindamycin (**3**).

The second part of this paper relates to the bound conformations. Transferred NOESY (TRNOESY) experiments were proved to be efficient for the location and detection of weak interactions due to ribosomal activity, providing a means to study the relationship between the conformation of antibiotics when interacting and their activity. We previously carried out a study on the antibiotic–ribosome weak interactions with *E. coli* ribosomes of the 14- and 16-membered macrolides,[2,11–13] the new class of antibiotics called ketolides[14–16] and the lincosamides.[17] We propose now to analyse whether the active molecules belonging to the MLS_B classes present a shared bound region[17] when weakly bound to *E. coli*, *S. pneumoniae* and *S. aureus* ribosomes.

Results and discussion

1 Dissociation equilibrium constant, K_D

Consider a ligand, A (Antibiotic), which binds to a macromolecule, R (Ribosome), to form a 1:1 complex A–R. The single equilibrium binding process is illustrated in eqn. (1)

$$A + R \underset{k_{off}}{\overset{k_{on}}{\rightleftharpoons}} A\text{–}R \qquad (1)$$

where [A] is the aqueous antibiotic concentration, [R] is the binding site concentration, [AR] is the bound antibiotic concentration. The dissociation constant, K_D, is defined by eqn. (2). The bound antibiotic mole fraction is defined by eqn. (3), provided that the free antibiotic concentration is in large excess over the bound antibiotic concentration.

$$K_D = \frac{[A][R]}{[AR]} = \frac{k_{off}}{k_{on}} \qquad (2)$$

$$a_b = \frac{[AR]}{[A]} \qquad (3)$$

All the fast-exchange NMR parameters can be cast in the following form [eqn. (4)] where a_f is the antibiotic mole fraction

$$P_{obs} = a_f P_f + a_b P_b \qquad (4)$$

that is free and a_b the fraction that is bound, ($a_f + a_b = 1$). The fast-exchange NMR parameters, P, can be $\Delta\nu$, $\Delta\delta$, $1/T_2$ or $1/T_1$, while P_f and P_b are the corresponding parameters of the free and bound states, respectively. By combination of eqns. (2)–(4) which can be simplified for a large excess of the free ligand,[18,19] $[A] \approx [A]_T$, we obtain eqn. (5). The variation of

$$\frac{[R]_T}{(P_{obs} - P_f)} = \frac{[A]_T + K_D}{(P_b - P_f)} \qquad (5)$$

$(P_{obs} - P_f)$ as a function of $[A]_T$ (with $[R]_T$ constant) can be analysed in terms of two unknowns $(P_b - P_f)$ and K_D. Thus, a plot of $[R]_T/(P_{obs} - P_f)$ *versus* $[A]_T$ allows $1/(P_b - P_f)$ to be obtained from the slope and $K_D/(P_b - P_f)$ from the intercept on the *y*-axis (Fig. 2a). The equilibrium binding constant K_D can be determined from the behaviour of any one of the observable NMR parameters.[18,19]

Evidence for ribosome–antibiotic interactions can be seen in the binding-induced line broadening in the NMR spectra of the antibiotic, and the binding constant K_D can be determined, according to eqn. (5) with $P_{obs} = \Delta\nu_{obs}$. The measurement of the dissociation equilibrium constant for weak interaction with ribosomes, by the line broadening method, was only worthwhile when a fast exchange seemed to prevail.[20,21] When the experiments were performed with *E. coli* 70S ribosomes (0.8 μM), the binding-induced line broadening increased as a function of the ligand concentration (the ratio of antibiotic to ribosome varied from 600 to 3000). From these linear plots, we obtained the low affinity dissociation constant values (±10%), $K_D = 2.1 \times 10^{-3}$ (telithromycin), 3.4×10^{-3} (roxithromycin) and 6.0×10^{-3} (clindamycin). With *S. aureus* ribosomes, the broadening data did not allow a reliable determination of the binding constants as a result of the difficulty in measuring the intrinsic resonance line widths. The selective T_2 relaxation times were preferred to assess the binding of antibiotics to *E. coli*, *S. pneumoniae* and *S. aureus* ribosomes. The method based on the measurement of T_2 (CPMG) gave values of K_D in the same range as the line broadening method.

1.1 T_2 (CPMG) method. The Carr–Purcell–Meiboom–Gill (CPMG) spin-echo decay rate was used to estimate the rate of dissociation of the antibiotic–ribosome complexes. If the chemical exchange rate is fast with respect to the chemical shift difference ($\delta\omega = \delta_b - \delta_f$) the two signals coalesce to form a single resonance. The observed relaxation rate ($1/T_{2obs}$) equals the weighted average of both the relaxation rates of the free ($1/T_{2f}$) and bound [$1/(T_{2b} + \tau_b)$] ligands [eqn. (6)] where T_{2b} is

$$\frac{1}{T_{2obs}} = \frac{a_f}{T_{2f}} + \frac{a_b}{T_{2b} + \tau_b} \qquad (6)$$

the transverse relaxation time, τ_b the exchange lifetime of the bound antibiotics, and T_{2f} equalled the observed antibiotic T_2 in buffer.

In the case of fast exchange, $\tau_b < T_{2b}$, while for the slow-exchange limit where $\tau_b > T_{2b}$,

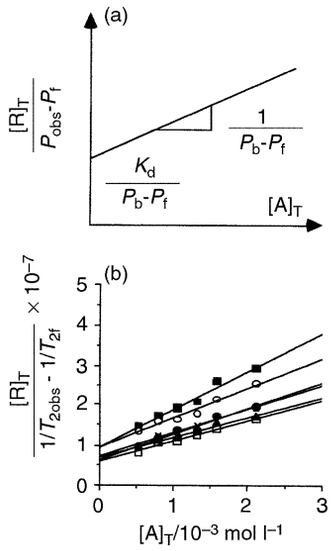

Fig. 2 (a) The binding constant K_D can be obtained from the vertical intercept of a linear titration plot of eqn. (5) as a function of the concentration of the binding ligand. The fast-exchange NMR parameters, P_{obs}, can be $\Delta\nu$, $\Delta\delta$, $1/T_2$ or $1/T_1$; (b) plots obtained with eqn. (5) ($1/T_{2obs}$) for telithromycin with *E. coli* (0.8 μM). (▲) 6-Me, (□) 12-Me, (×) 6-OMe, (○) 2-Me, (●) 10-Me, (■) 3′-N(Me)$_2$.

$$\frac{1}{T_{2obs}} = \frac{\alpha_f}{T_{2f}} + \frac{\alpha_b}{T_{2b}} \quad (7)$$

$$\frac{1}{T_{2obs}} = \frac{\alpha_f}{T_{2f}} + \frac{\alpha_b}{\tau_b} \quad (8)$$

1.1.1 Temperature dependence. One experimental way to distinguish between slow and fast exchange is to measure the temperature dependence of the spin–spin relaxation time[22] or the line width of the exchanging nuclei.[23] If there is no chemical shift difference between the two sites, the observed relaxation rate $1/T_{2obs}$ is described by eqn. (6). For the fast exchange ($T_{2b} > \tau_b$), the resonance lines will narrow with increasing temperature as the transverse relaxation time of the bound ligands, T_{2b}, increases with temperature.[20–22] In the slow-exchange limit ($T_{2b} < \tau_b$), on the other hand, the opposite situation prevails, and the line width ($1/\pi T_2$*) will increase with the temperature as the exchange lifetime of the bound ligand, τ_b, invariably decreases with the rise in temperature.

We investigated the effect of temperature on the exchange with 0.8 (*E. coli*), 0.4 (*S. pneumoniae*) and 0.2 (*S. aureus*) μM ribosomal concentration and with 1 mM fraction of antibiotics. In the case of telithromycin and roxithromycin in interaction with *E. coli* and *S. pneumoniae* ribosomes, fast exchange prevails, while in experiments with *S. aureus* ribosomes, we observe the antibiotic–ribosome complexes in intermediate exchange.[21] The slow-exchange limit prevails for the antibiotics–*S. aureus* ribosomes interaction and similarly for the clindamycin–ribosome (*E. coli*, *S. pneumoniae* and *S. aureus*) interaction.

The approach developed in this study for the measurements of equilibrium dissociation constants can be used with the limitation that a deviation from fast exchange can introduce significant errors in the measured binding parameters.[20] The lineshape analysis is difficult to perform in these kind of experiments since the line width of the resonances from the complexes is too large. In practice, in cases of intermediate exchange where a single resonance is observed at a particular frequency, the assumption of fast exchange is usually made to facilitate the analysis.

1.2 Equilibrium binding constant. K_D values were estimated (±10%) from the vertical intercept of the titration plots

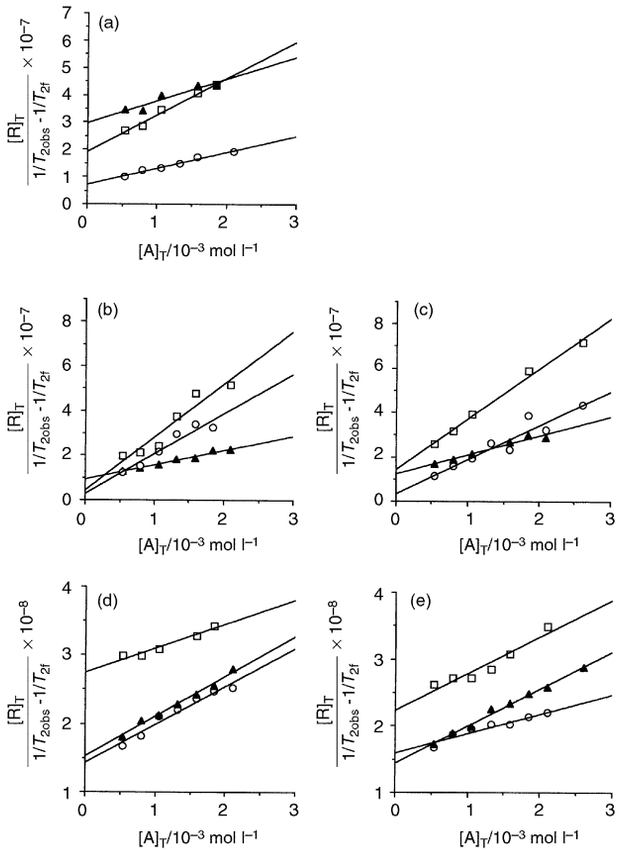

Fig. 3 Comparison of plots [eqn. (5)] for telithromycin, (○) 6-OMe, roxithromycin, (□) 3″-Me and clindamycin, (▲) S-Me, binding to ribosomes: (a) *E. coli* (0.8 μM); (b) erythromycin-sensitive and (c) -resistant *S. pneumoniae* (0.4 μM); (d) erythromycin-sensitive and (e) -resistant *S. aureus* (0.2 μM).

according to eqn. (5), and are reported in Table 1. The initial antibiotic ligand concentration was 0.5 mM, and increments of added ligand varied in the range of a few millimolars, while the ribosome concentrations were 0.8 (*E. coli*), 0.4 (*S. pneumoniae*) or 0.2 (*S. aureus*) μM. No chemical shift was observed upon addition of the ribosomes.

The antibiotic concentration dependence of the observed T_2 was examined using a fast CPMG pulsing rate ($1/\tau_{cp} = 500$ s^{-1}) to which the refocusing 180° pulses of the Carr–Purcell sequence were applied. Since the fast pulsing rate eliminated chemical exchange contributions to relaxation, the observed T_2 reflected the weighted average of the antibiotic relaxation rates in the bound and free states [eqn. (6)]. Although desirable for the present study, it was not possible to obtain data at faster pulsing rates because of limitations imposed by the recovery characteristics of our instrument. In buffer the average T_{2f} values for methyl signals showed no dependence on antibiotic concentration (Table 1). With increasing antibiotic concentration, the resulting relaxation time T_{2obs} also increased (Fig. 2b) because α_b progressively decreased (and α_f increased) as the low affinity binding sites became occupied.[8]

Several mechanisms can cause antibiotic relaxation enhancement upon binding to the ribosome. Two experiments should indicate that the relaxation enhancement is caused by the binding of the antibiotics to the ribosome in the binding site according to eqn. (1), and not by viscosity increase or non-specific binding:[22] (i) the plots of T_{2obs} *versus* antibiotic concentration (Fig. 2b), keeping the ribosome concentration constant (see below), clearly indicate that the line broadening is caused by the binding of the antibiotics to the ribosome. A straight line is obtained in accordance with eqn. (5) (Fig. 3); (ii) the effect observed in the NMR relaxation of an antibiotic induced by

Table 1 K_D values and transverse relaxation times ($T_{2b} + \tau_b$) of the bound ligands, determined by measuring T_2 (CPMG) of well-resolved methyl signals for the weak interaction of **1**–**3** antibiotics at bacterial ribosomes (*E. coli* and erythromycin-sensitive and -resistant *S. pneumoniae* and *S. aureus*)

		Ribosomes[a]									
		E. coli		*S. pneumoniae*				*S. aureus*			
				Erythromycin-sensitive		Erythromycin-resistant		Erythromycin-sensitive		Erythromycin-resistant	
	Buffer										
Signals	T_{2f}/ms	$T_{2b} + \tau_b$/μs	K_D[b]	$T_{2b} + \tau_b$/μs	K_D[b]	$T_{2b} + \tau_b$/μs	K_D[b]	$T_{2b} + \tau_b$/μs	K_D[b]	$T_{2b} + \tau_b$/μs	K_D[b]
Telithromycin (**1**)											
3′N(Me)$_2$	240	95	1.1×10^{-3}	220	4.5×10^{-5}	240	2.8×10^{-4}	7	2.4×10^{-3}	5	4.6×10^{-3}
6-OMe	305	59	1.2×10^{-3}	150	2.4×10^{-4}	180	7.3×10^{-4}	6	2.6×10^{-3}	3	5.5×10^{-3}
12-Me	180	50	1.2×10^{-3}	110	5.4×10^{-4}	120	1.2×10^{-3}	3	4.7×10^{-3}	3	4.8×10^{-3}
2-Me	363	75	1.2×10^{-3}	130	5.3×10^{-4}	190	9.1×10^{-4}	6	3.3×10^{-3}	4	4.9×10^{-3}
6-Me	153	50	1.4×10^{-3}	120	5.8×10^{-4}	160	7.4×10^{-4}	4	3.1×10^{-3}	3	5.3×10^{-3}
10-Me	268	63	1.0×10^{-3}	180	9.0×10^{-5}	160	4.3×10^{-4}	6	2.8×10^{-3}	[c]	[c]
Average	251	65	1.2×10^{-3}	152	3.4×10^{-4}	175	7.1×10^{-4}	5	3.1×10^{-3}	4	5.1×10^{-3}
Roxithromycin (**2**)											
3″O-Me	372	[c]	[c]	180	7.6×10^{-4}	230	6.7×10^{-4}	4	8.0×10^{-3}	6	5.0×10^{-3}
3′N(Me)$_2$	183	185	9.4×10^{-4}	270	2.6×10^{-4}	160	1.5×10^{-3}	6	5.0×10^{-3}	6	4.9×10^{-3}
6-Me	143	121	1.4×10^{-3}	180	5.8×10^{-4}	330	2.1×10^{-4}	2	1.2×10^{-2}	2	1.3×10^{-2}
3″-Me	277	134	1.5×10^{-3}	240	1.9×10^{-4}	230	6.3×10^{-4}	3	7.8×10^{-3}	6	4.0×10^{-3}
10-Me	261	145	1.3×10^{-3}	340	2.4×10^{-5}	350	2.2×10^{-4}	5	6.7×10^{-3}	[c]	[c]
Average	247	146	1.3×10^{-3}	242	3.6×10^{-4}	260	6.5×10^{-4}	4	7.9×10^{-3}	5	6.7×10^{-3}
Clindamycin (**3**)											
1′-Me	299	20	1.2×10^{-2}	70	1.4×10^{-3}	90	1.2×10^{-3}	4	3.2×10^{-3}	3	5.4×10^{-3}
S-Me	687	27	1.2×10^{-2}	60	1.5×10^{-3}	90	1.4×10^{-3}	5	2.7×10^{-3}	6	2.6×10^{-3}
8-Me	283	19	1.7×10^{-2}	70	1.1×10^{-3}	80	1.3×10^{-3}	5	3.1×10^{-3}	4	4.6×10^{-3}
3″-Me	776	49	9.8×10^{-3}	90	1.5×10^{-3}	90	1.6×10^{-3}	8	2.6×10^{-3}	9	2.7×10^{-3}
Average	511	29	1.3×10^{-2}	70	1.4×10^{-3}	90	1.4×10^{-3}	6	2.9×10^{-3}	5	3.8×10^{-3}

[a] The antibiotics **1**–**3** were tested with *E. coli* ribosomes (0.8 μM), with erythromycin-sensitive and erythromycin-resistant *S. pneumoniae* (0.4 μM) and *S. aureus* ribosomes (0.2 μM). [b] Estimated error: ±10%. [c] Low resolution.

binding interaction with ribosomes is specific when competitive antibiotic displacement is observed[19,22] in a series of measurements in which the inhibitor antibiotic is added gradually to a solution containing antibiotic and ribosome (Fig. 4).

1.2.1 E. coli ribosomes. Antibiotics were added to *E. coli* ribosomes at molar ratios (antibiotic–ribosome) ranging from 600 to 2600. The antibiotic protons relaxed slower (enhanced T_{2obs}) with a relative increase in antibiotic concentration (Fig. 2b). Fig. 3a shows titration plots of the observed selective T_{2obs} of the 6-OMe, the 3″-Me and the S-Me protons of telithromycin, roxithromycin and clindamycin, respectively. In 0.8 μM *E. coli* ribosome solution, antibiotic concentration dependence was evident (Figs. 2b, 3a, S1 and S2). The linearity of the plots illustrates the binding of the antibiotics to the bacterial ribosomes according to eqn. (1).

The binding constant K_D can thus be obtained from the *y*-intercept of the linear plot; for telithromycin, roxithromycin and clindamycin binding to the *E. coli* ribosomes, $K_D = 1.2 \times 10^{-3}$, 1.3×10^{-3} and 1.3×10^{-2}, respectively (Table 1). The value of K_D was closely related to the antibacterial activity. Telithromycin (**1**) displayed a significantly better overall antibiotic activity[16] than did clindamycin (**3**),[16] and at the same time, the $K_{D(1)}/K_{D(3)}$ ratio (Fig. 4a) was in the range of 0.1–0.2 for their weak *E. coli* ribosomal interaction.

A value for ($T_{2b} + \tau_b$) can be determined from the slope (Table 1). Antibiotic binding to *E. coli* represented a significant immobilisation of the molecules as revealed by ($T_{2b} + \tau_b$), for example 65 μs for telithromycin. The temperature dependence of the NMR broadening is consistent, as discussed above, with the exchange lifetime of bound telithromycin τ_b which is shorter than its relaxation time T_{2b}. Since $\tau_b = k_{off}^{-1}$, where k_{off} is the dissociation rate constant of the ribosome–antibiotic complex, we can derive a lower limit of $k_{off} > 1.5 \times 10^4$ s^{-1}. As the dissociation constant K_D of the lower affinity sites equals k_{off}/k_{on}, it allows an evaluation of $k_{on} > 1.2 \times 10^7$ for telithromycin. This is different for the loosely bound clindamycin: the τ_b value was determined (29 μs) and $k_{on} \approx 2.6 \times 10^6$ M^{-1} s^{-1}.

The study directly demonstrates the ability of MLS_B antibiotics to discretely bind to ribosomes when the high affinity antibiotic binding is biologically observed. As evidenced from the values of its dissociation equilibrium constant (K_D) for low affinity and its net relaxation ($T_{2b} + \tau_b$) due to the interaction with ribosomes, the results suggest that telithromycin displayed a higher affinity for weak *E. coli* ribosomal interaction than the other tested antibiotics.

1.2.2 S. pneumoniae ribosomes. In this series of measurements, the ribosome concentration was reduced from 0.8 μM (*E. coli*) to 0.4 μM. A similar plot for MLS_B antibiotics with the erythromycin-susceptible and -resistant *S. pneumoniae* ribosomes is given in Figs. 3b, c and 4b. A straight line is again obtained in accordance with eqn. (5). Thus the dissociation constant can be obtained for the ligands binding to the *S. pneumoniae* ribosomes (Table 1); for example, $K_D = 3.4 \times 10^{-4}$ for telithromycin and 1.4×10^{-3} for clindamycin (results with sensitive strains).

Using the experimental plots according to eqn. (5), one can calculate ($T_{2b} + \tau_b$) (Table 1) the spin–spin relaxation time T_{2b} and evaluate the average residence time of the bound ligand. The clindamycin k_{off} value ($\approx 1 \times 10^4$ s^{-1}) is more than 2 times higher than those determined for telithromycin and roxithromycin ($>4 \times 10^3$ s^{-1}). Assuming a simple A + R $\rightleftharpoons$ A–R mechanism, the lower limit of the association rate constant k_{on} can be calculated; $k_{on} \approx 1.0 \times 10^7$ M^{-1} s^{-1} for telithromycin, and 1.0×10^6 M^{-1} s^{-1} for clindamycin.

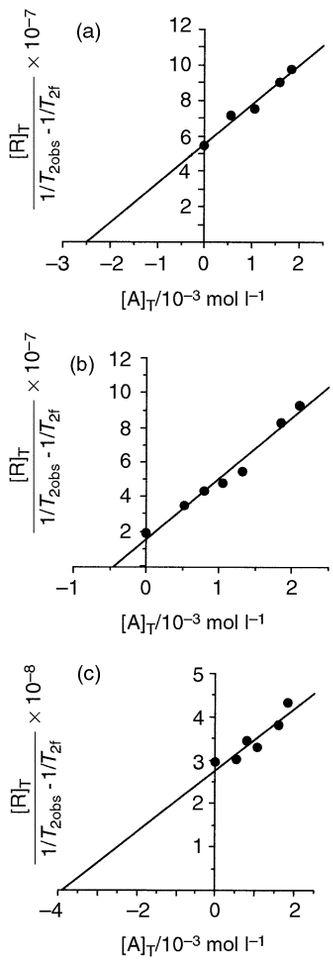

Fig. 4 Competitive titration plots for clindamycin, (●) 3″-Me, with telithromycin according to equation:[19,22] $[R]_T/(1/T_{2obs} - 1/T_{2f}) = [A]_I (T_{2b} + \tau_b)[K_{D(L)}/K_{D(I)}] + [1/(T_{2b} + \tau_b) - 1/T_{2f}][K_{D(L)} + [A]_L]$ where $K_{D(I)}$ is the dissociation constant of the competing ligand (**I**). A straight line is obtained upon the plot of $[R]_T/(1/T_{2obs} - 1/T_{2f})$ *versus* $[A]_I$. The slope, $(T_{2b} + \tau_b)[K_{D(L)}/K_{D(I)}]$, simplified since $T_{2f} \gg (T_{2b} + \tau_b)$, directly provides the value of $K_{D(L)}/K_{D(I)}$ which matches well the ratio found by T_2 (CPMG) experiments (see Table 1); (a) with *E. coli* ribosomes (0.8 μM), $K_{D(L)}/K_{D(I)} \approx 0.2$ ($K_{D(I)}/K_{D(3)} = 1.2 \times 10^{-3}/1.3 \times 10^{-2} \approx 0.1$); (b) with *S. pneumoniae* ribosomes (0.4 μM), $K_{D(L)}/K_{D(I)} \approx 0.2$ ($K_{D(I)}/K_{D(3)} = 3.4 \times 10^{-4}/1.4 \times 10^{-3} \approx 0.2$), and (c) with *S. aureus* ribosomes (0.2 μM), $K_{D(L)}/K_{D(I)} \approx 1.1$ ($K_{D(I)}/K_{D(3)} = 3.1 \times 10^{-3}/2.9 \times 10^{-3} \approx 1.1$).

This is in agreement with the observation of biological activity.[16] Susceptibility of *pneumococci* to telithromycin (erythromycin-susceptible and -resistant) was tested and results were compared with those of other compounds belonging to the MLS_B class of antimicrobial agents. Telithromycin was very active against the strains tested.[24,25]

1.2.3 S. aureus ribosomes. Similar experiments were carried out with erythromycin-sensitive (Figs. 3d and 4c) and -resistant (Fig. 3e) strains of *S. aureus* ribosomes but the concentration of the ribosomes was 0.2 μM since a more pronounced broadening did not allow a reliable determination of the binding constants (Table 1) due to the limited sensitivity of the NMR signals.

When antibiotic binding to sensitive strains of *S. aureus* was analysed, there was little change in T_2 with increasing antibiotic concentration. This was expected in the case of lower-affinity binding, since α_b changed very little when binding sites could not be appreciably filled over the antibiotic concentration range. Similarly, antibiotic binding to resistant strains of *S. aureus* showed little dependence on antibiotic concentration. Indeed, the direct NMR titration experiments produced titration plots with slopes close to zero. Negligible interactions of antibiotics with *S. aureus* ribosomes were demonstrated by the observed T_2 values which were not very far from T_2 of the free antibiotics, as expected for very loose complexes. The experimental plots directly yielded the sum of T_{2b} and τ_b equal to 5 ± 1 μs. The lower affinity binding represented a marked decrease in the measured lifetime τ_b and $k_{off} = 1/\tau_b \approx 20 \times 10^4$ s^{-1}.

The telithromycin K_D value (3.1×10^{-3}) is more than 2 times lower than the roxithromycin K_D value (7.9×10^{-3}), for example. The results were related to the activity (MIC) values[16,26] of these antibiotics against sensitive *S. aureus* strains (0.04 and 0.6 μg ml^{-1} for telithromycin and roxithromycin, respectively). Telithromycin K_D (5×10^{-3}) measured with resistant *S. aureus* strains is different and its affinity is lower (MIC ≈ 40 μg ml^{-1}).[16]

The results presented here demonstrate that T_2 measurements are useful for measuring the specific binding of antibiotics to bacterial ribosomes in their low-affinity state. The results show that the binding constants are in agreement with results from high-affinity binding assays (in the order telithromycin > roxithromycin and clindamycin). This method works well when the ligand has fast dissociation kinetics. This is recognised as a particularly difficult regime in which it is not easy to measure K_D by other methods.

2 Transferred nuclear Overhauser effects

As the MLS_B antibiotic family exchanges very rapidly between the free and the bound state, only the TRNOE-derived distances are appropriate to calculate their ribosome-bound structures.[2,11–14,17,27,28] Upon the addition of ribosomes, in the TRNOESY experiment, a high number of negative cross peaks demonstrated the interaction of the antibiotics with ribosomes. Internuclear distance information was obtained by the evaluation of cross-peak volumes (Tables S1–S3), and interproton distances were set as follows: 2–3 Å, strong (s), 3–4 Å, medium (m) and 4–5 Å, weak (w).

2.1 Bound structures. The ribosome-bound conformations of the antibiotics were determined by molecular dynamics calculations incorporating transferred NOE distance constraints.

2.1.1 Telithromycin bound conformations. Two structures represented the *E. coli* bound state of the drug: S$^-$-(*Z*)-**AD2C3** (Fig. 5a), the predominant structure generated during the dynamics protocols with TRNOE-distance constraints, and S$^-$-(*Z*)-**BD1C3** (Fig. 5b), the major free conformation.[14] Two types of conformation were found for telithromycin. Type **A** [H(4)–C(4)–C(5)–H(5), *eclipsed*] corresponds to 3-CO "*exo*" with H(4) 'folded in' and Me(4) 'down', and type **B** [H(4)–C(4)–C(5)–H(5), *trans*] to 3-CO "up" with H(4) 'down' and Me(4) 'folded out'. They might be compared to **A** and **B** as found in erythromycin derivatives: the C(3)–C(5) 'folded-out' termed **A**, and the inward folding of the C(3) fragment in **B** with the cladinose unit rising above the macrocycle.[29,30] The desosamine sugar adopts a perpendicular orientation to the macrocyclic lactone ring corresponding to the **D1** and **D2** conformations. The alkyl part of the chain, the C(20)–N(20) dihedral angle, is g^- (S$^-$) and the imidazolyl-pyridine part of the chain, the C(23)–C(28) torsion angle, is *eclipsed* S-(*Z*). The **C3** chain is characterised by the stacking of the imidazole and pyridine units with both carbonyl CO(1) and CO(3).

The bound structures of telithromycin in weak interaction with *S. pneumoniae* (Fig. 5c) and with *S. aureus* ribosomes (Fig. 5d) were blocked into a specific and favoured **BD1C2** conformation derived from TRNOE investigations. Some TRNOEs expected for models **A** were missing, particularly the connectivities {6-OMe}13, {12-Me}Me(4) and especially {11}4 present in the *E. coli* bound structure. The imidazolyl-pyridine part of the chain is *eclipsed* S-(*Z*) and *anti* S-(*E*) in the *S. pneumoniae* and *S. aureus* bound structures, respectively. The spatial proximities observed from imidazole protons {H(21) and H(23)} and from pyridine protons {H(25)–H(28)} referred

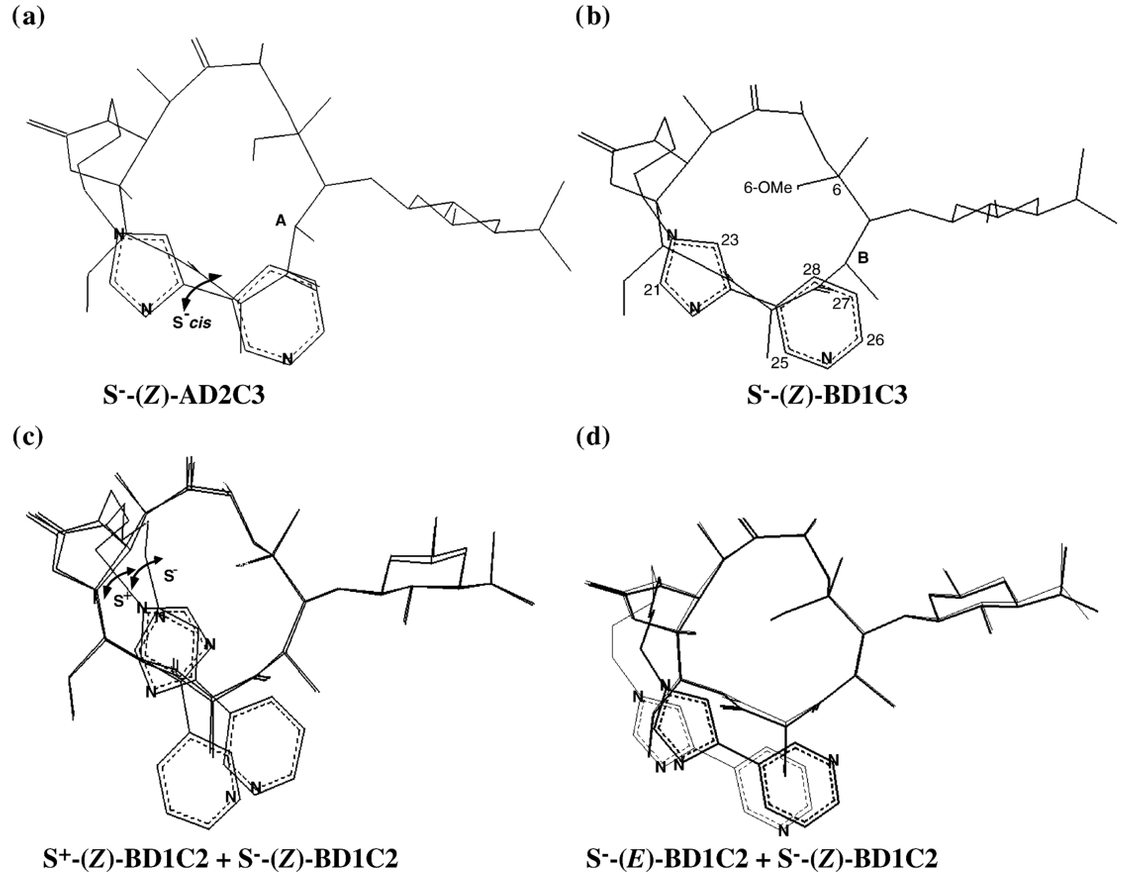

Fig. 5 The structures are referred to as S^+ or S^- when the C(18)–C(21) rotor of the alkyl part of the chain is either g^- (S^-) or g^+ (S^+) and, as S-(*Z*) or S-(*E*) when the two nitrogen atoms of the imidazolyl-pyridine part of the chain C(23)–C(28) are either *eclipsed* or *anti*. (a) Telithromycin bound structures at *E. coli* ribosomes: S^--(*Z*)-**AD2C3** and (b) S^--(*Z*)-**BD1C3**. (c) Superimposition of telithromycin bound structures at erythromycin-sensitive and -resistant *S. pneumoniae* ribosomes, S^+- (in bold) and S^--(*Z*)-**BD1C2**. (d) Superimposition of telithromycin bound structures at erythromycin-sensitive and -resistant *S. aureus* ribosomes, S^--(*E*)- (in bold) and S^--(*Z*)-**BD1C2**.

preferentially to a **C2** chain stacked only with CO(1). The inter desosamine-chain TRNOEs, {5′-Me}26 and {5′-Me}27, which induced the **C3** chain conformation in the *E. coli* bound state, were non-existent in the *S. pneumoniae* and *S. aureus* complexes.

The main difference between *E. coli* and *S. pneumoniae*, *S. aureus* telithromycin bound structures was the conformational change in the imidazolyl-pyridine chain in the macrocycle and in the desosamine ring (Fig. 5). This is of particular interest since it could be related to the biological activity of telithromycin. The ketolide has more affinity than the macrolide and the lincosamide tested against *S. pneumoniae* and *S. aureus* strains.

2.1.2 Roxithromycin bound conformations. The TRNOE data suggested that a similar **AD1** roxithromycin conformation binded to *E. coli* and *S. aureus* ribosomes. In the *E. coli* ribosome complex (Fig. 6a) the macrocyclic lactone ring corresponded to the C(3)–C(5) 'folded-out' **A** conformation similar to the **A** ketolide.[29,30] The two sugar rings presented the **D1** conformation perpendicular to the macrocycle. The far sugar-chain TRNOE observed from OMe(19) showed the end of the oxime chain close to the joining part of the cladinose sugar. In the *S. aureus* complex (Fig. 6b) the new far TRNOE observed from OMe(19) to Me(3″) and the new {5″-Me}H(5′) and {5″}Me(5′) TRNOEs were due to a relative change of the cladinose orientation and a stretching out of the oxime chain. With *S. pneumoniae* ribosomes, roxithromycin also gave rise to the **A** macrocycle conformation and to **D1** and **D3** desosamine ring orientations (Fig. 6a). Some mobility around the glycosidic bonds is sufficient to induce the **D3** coplanar conformation.

The plausible roxithromycin bound structure relative to the weak specific binding to the different bacterial ribosomes corresponds to the **AD1** conformation. That may be of importance for the roxithromycin mode of action as its activity was markedly decreased with *S. aureus* ribosomes compared to the **BD1** telithromycin bound structure. The constant K_D obtained for roxithromycin binding to *S. aureus* ribosomes is more than 2 times higher than for telithromycin.

2.1.3 Clindamycin bound conformations. The clindamycin bound structure (Fig. 6d) at *E. coli* and *S. aureus* ribosomes corresponded to the **G1P2C2** conformation (Fig. 6d).[17] The TRNOE spectra of clindamycin with *S. aureus* contain most of the crosspeaks that were observed with *E. coli* ribosomes. This confirmed the tendency of the Cl atom to favour the most stable **G1** conformation of the *galacto*-octopyranoside.[17] No change is involved in the *envelope* **P2** of the pyrrolidine group and in the **C2** propyl chain. The 3″-Me group of the chain ends spatially proximate to the 8-Me of the *galacto*-octopyranoside, thus leading to a folded conformation allowing interaction with the *S. aureus* receptor. On the other hand, the privileged **G2P2C1** bound structure (Fig. 6c) at *S. pneumoniae* ribosomes is characterised by a different spatial location of the Cl atom, and the 8- and 3″-Me groups. This may be correlated with the antibacterial activity of clindamycin since its K_D for weak binding to *S. pneumoniae* ribosomes is about 4 times higher than the K_D of telithromycin (Table 1).

2.2 Binding surface. The most obvious evidence for ribosome–antibiotic interactions is the binding-induced differential line broadening in the NMR spectra of the free ligands (Fig. S3). In particular, the broadening observed may reflect proximity to a binding surface.

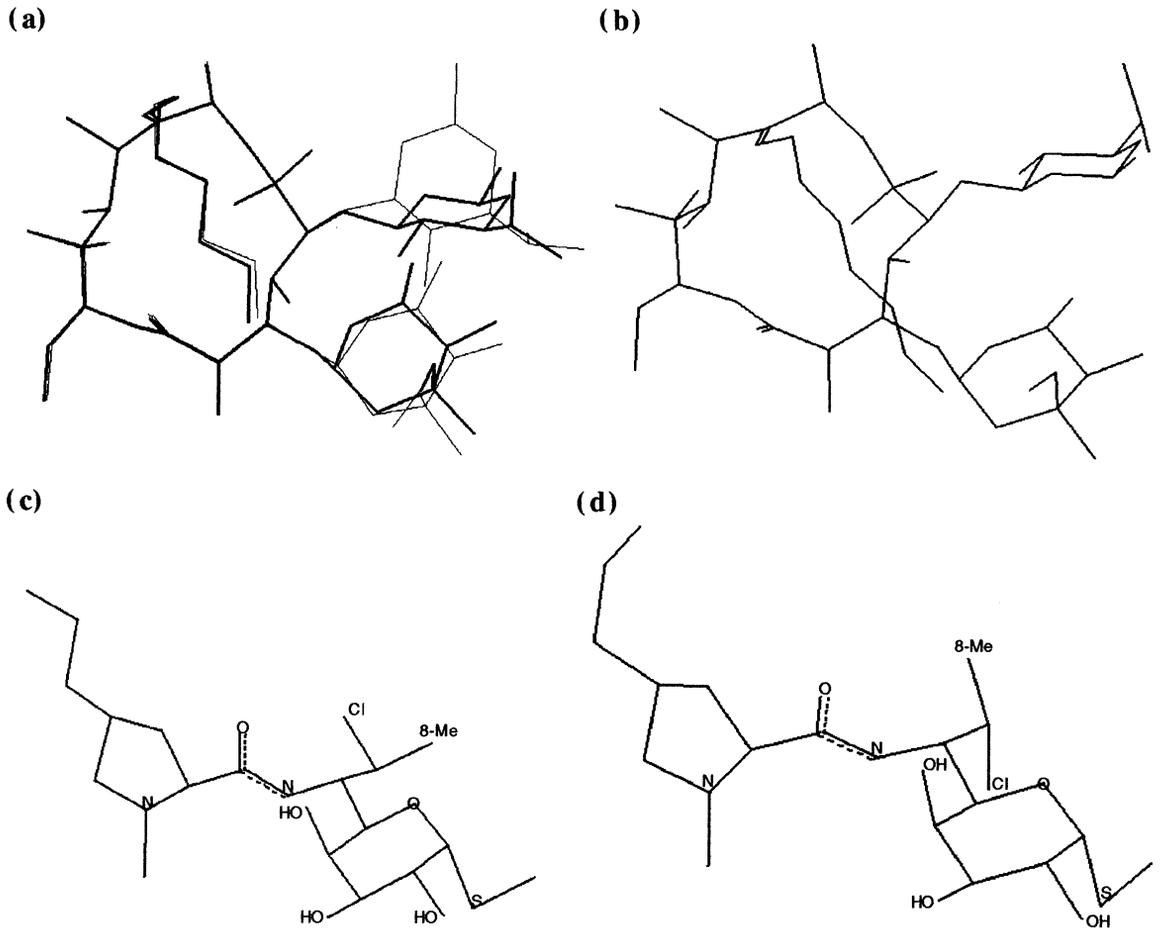

Fig. 6 (a) Superimposition of roxithromycin bound structures at *E. coli*, erythromycin-sensitive (**AD1**, in bold) and -resistant (**AD3**) *S. pneumoniae* ribosomes; (b) roxithromycin bound structure (**AD1**) at *S. aureus* ribosomes; (c) clindamycin bound structure (**G2P2C1**) at *S. pneumoniae* ribosomes; (d) clindamycin bound structure (**G1P2C2**) at *E. coli* and *S. aureus* ribosomes.

It is interesting to notice that each MLS_B antibiotic weakly binds to ribosomes at an almost identical 'surface' of the drug molecule, independently of the ribosome strains. For telithromycin and roxithromycin bound structures, the hydrogen atoms giving the most extensively broadened resonances correspond to the C(10-Me)–C(12-Me)–C(15-Me)–O(14)–C(2-Me)–C(6-Me) region of the macrocycle ring. The broadening is also observed in telithromycin C(23)–C(27), C(3′-$N(Me)_2$)–C(5′-Me) region and in roxithromycin oxime chain (19-OMe) and cladinose sugar unit C(2″)–C(3″-Me)–C(4″) except for *S. aureus* ribosomes. For clindamycin, the broadening was observed in the N(H)–C(O)–C(2′)–C(3′)–C(5′) proline unit and the methyl Me(3″), Me(8) region, except for the 3′-pyrrolidine region at the *S. pneumoniae* ribosomes.

Since the specific broadening of each antibiotic upon binding was about the same in the different bacterial ribosomes tested here, it can be concluded that their mode of weak binding was similar. The fact that erythromycin resistance due to A2058 in domain V of 23S rRNA, at the catalytic centre of the peptidyl transferase,[31] is not necessarily associated with the weak interaction detected by NMR spectroscopy, favours the model that ketolide, macrolide and lincosamide weakly interact on sites which could partially overlap even if the antibiotics act strongly on different sites. All this is in agreement with a low-affinity binding level distinct from the tight inhibition binding one.

2.2.1 A fragment shared by MLS antibiotics. The superimposition of the C(6)–C(2′) binding region of clindamycin (the amide CO and α-N) with the bottom part C(2)–C(13) of the telithromycin and roxithromycin macrolactone ring (the ester CO and α-O) displays conformational similarities (Fig. 7). The superimposition of the MLS antibiotic bound structures revealed that clindamycin places its 8-Me in the same spatial location as the 15-Me of telithromycin and roxithromycin (Fig. 7), except for *S. pneumoniae* ribosomes (Fig. 7b).

This is of particular interest since it could be related to the biological properties of these molecules, as competitive inhibition occurs between the various MLS drugs.[32] These antibiotics likely share a common *E. coli*[17] and, to a lesser degree, a *S. aureus* ribosomal binding surface since it is possible to relate C(3), C(4), C(5), C(6), C(7), C(Me8), N(H), C(O), C(2′) and N(1′) of clindamycin with C(10), C(11), C(12), C(13), C(14), C(Me15), O(14), C(O), C(2) and C(3) of telithromycin and roxithromycin (Fig. 7). The conformation of this fragment seems to be interesting for the antibiotic–ribosome recognition sites and it would be a plausible pharmacophore.

2.2.2 Antibiotic–E. coli complex. The **AD2C3** telithromycin bound structure relative to the weak binding to the *E. coli* ribosome shows conformational homology after superimposition with the **AD1** roxithromycin bound structure (Fig. 7a). The **A** conformation of the macrocycle seems to fit on the antibiotic–*E. coli* ribosome recognition site ($K_D = 1.2 \times 10^{-3}$ and 1.3×10^{-3} for telithromycin and roxithromycin, respectively). Superimposition of the bound structures (Fig. 7) revealed one change that may be of importance for the ketolide mode of action, namely a stretching out of the desosamine unit (**D2** compared to **D1**).

2.2.3 Antibiotic–S. pneumoniae and –S. aureus complex. The **BD1C2** conformation appeared to be the plausible telithromycin bound structure specific to the weak binding to the sensitive- and resistant-*S. pneumoniae* (Fig. 5c) and -*S. aureus* (Fig. 5d) ribosomes. This structure did not show conformational homology with the roxithromycin *S. aureus* bound

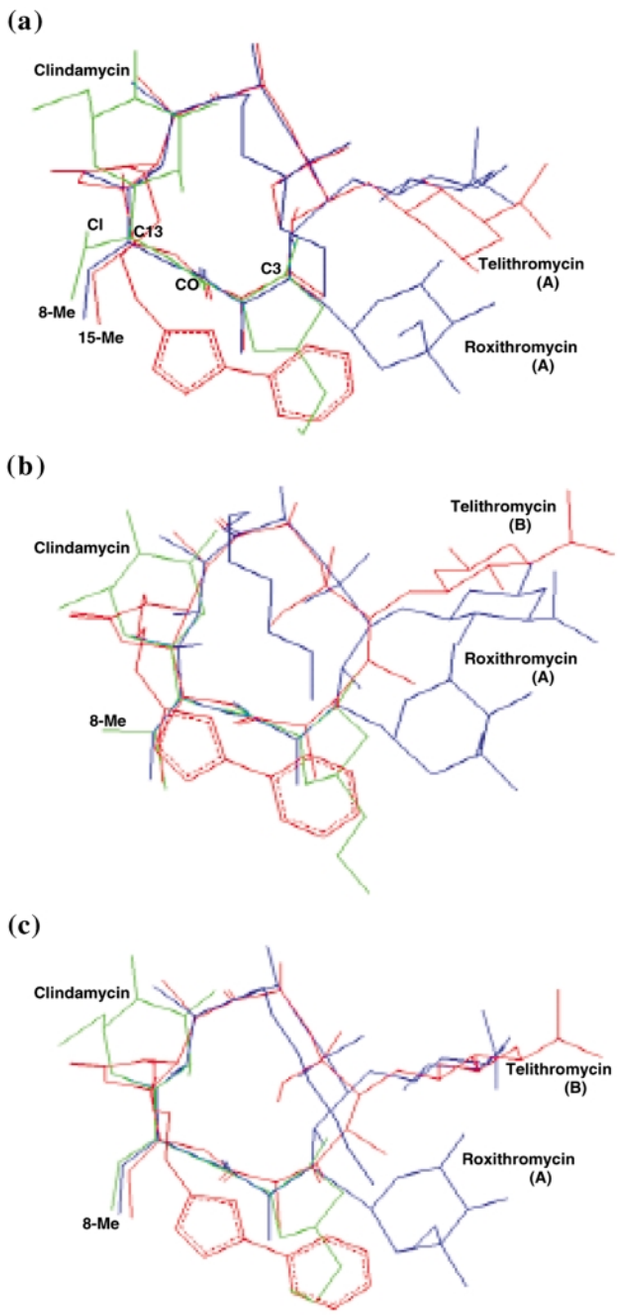

Fig. 7 Superimposition of the TRNOE bound structures for the three drugs, telithromycin (red), roxithromycin (blue) and clindamycin (green) at (a) *E. coli* ribosomes; (b) erythromycin-sensitive *S. pneumoniae* ribosomes; (c) erythromycin-sensitive *S. aureus* ribosomes.

structure (**AD1**) (Fig. 6b). The **B** conformation appeared as the conformation in weak interaction with *S. pneumoniae* and *S. aureus* ribosomes. The **B** conformation allowed telithromycin to obtain the desired profile of activity that resulted in a significant increase of activity against resistant strains. In the ketolides, the free space liberated by the cladinose was indicative of the importance of the cladinose area as well as the stacking of the aromatic chain in the interaction with the *S. pneumoniae* and *S. aureus* ribosomes.

Conclusion

The results presented here demonstrate that the NMR technique is sensitive, in a complex mechanism, in a step that cannot be measured adequately by the other methods. Results agree well with biological activity, and the approach has provided a means of estimating parameters not previously determined. This is the first time that the equilibrium binding constant K_D relative to the low-affinity pre-inhibition binding site has been estimated and the values are obtained with the T_2 (CPMG) method. The important broadening observed in the study with *S. aureus* ribosomes shows that for the weak binding of antibiotics the interaction was a slower exchange process compared with *S. pneumoniae* and *E. coli* ribosomes.

The K_D results show that the ketolide has more affinity for the weak interaction site of the bacterial ribosomes than the other antibiotics tested. The values of weak affinity are closely related to the activity of the MLS_B antibiotics against bacteria, thus providing a relationship between weak interaction and affinity. This can explain some of the significant differences between telithromycin and the other antibiotics.

This study also revealed an interesting relationship between the conformation of antibiotics when interacting and their activity. The telithromycin *S. pneumoniae* and *S. aureus* bound conformation did not present the same structural analogy as the structure relevant to the *E. coli* receptor, while for roxithromycin and clindamycin the *S. aureus* bound structures were identical to the *E. coli* bound one. The **A** conformation of the telithromycin keto aglycone and the **C3** stereochemistry of its aryl-alkyl side chain were probably adapted to the *E. coli* receptor, while the **B** conformation and the **C2** chain were beneficial with regard to the *S. pneumoniae* and *S. aureus* ribosomes. These modifications may be of importance for the ketolide mode of action. The better biological activity of ketolide antibiotics depends on many factors, and these may include their bound conformations.

Experimental

Materials

The *E. coli* MRE 600 ribosomes were prepared at Hoechst Marion Roussel (HMR) as described[33] by a tangential ultrafiltration technique. Both 70S ribosomal preparations from *S. aureus* Ery-S and Ery-R and *S. pneumoniae* Ery-S and Ery-R strains were obtained as described by Umejawa[34] and Swenden[35] respectively, with slight modifications. O11UC4 and 030MV4 (HMR) are *S. aureus* and *S. pneumoniae* sensitive to macrolides, and O11CB20 and 030CR18 (HMR) are MLS_B (methylation of A^{2058} in N-6) *S. aureus* and *S. pneumoniae* resistant to erythromycin and oxacilline, respectively.

NMR spectroscopy

The antibiotics were dissolved in an aqueous NaD_2PO_4–Na_2DPO_4 buffer (0.05 M), with KCl (0.2 M) at physiological apparent pH 7.6 at concentrations of 2.5 mM. The experiments were run at 500 MHz for ^1H, at 293 K, on a Bruker AMX 500 spectrometer equipped with a Silicon Graphics workstation. Presaturation of the solvent was used for all the 1D and 2D ^1H experiments with the *S. pneumoniae* and *S. aureus* ribosomes, and another presaturation of the tris-HCl was needed for all the experiments with the *E. coli* ribosomes.

Spin–spin relaxation (T_2) measurements[8,36] were made using the CPMG pulse sequence. A non-selective 90° pulse ($t_{90} \approx 30$ μs) was used to excite the sample, and multiple non-selective 180° refocusing pulses ($t_{180} \approx 60$ μs) to generate the echo train. τ_{cp} is the time between refocusing 180° pulses in the CPMG pulse train, which was fixed at 2 ms. The times between successive echo sequences ($d_1 = 4$ s) was greater than 4 times T_1 to assure sample equilibrium. Relaxation data were collected for an interval spanning at least 2–3 times the T_2 decay constant. The data (after 12 experiments) were plotted as a function of echo evolution time and fitted to a single exponential using a non-linear least-squares fitting program. T_2 values are reported as time constants of these exponentials.

^1H TRNOESY experiments were identical to those used in the earlier studies[2,11–14,17] of the macrolide–, ketolide– and lincosamide–*E. coli* ribosome complexes.

Molecular modelling

Studies and bound conformation determinations were conducted according to the earlier procedures.[2,11–14] The calculations were run on a Silicon Graphics computer using the CVFF Forcefield by Dauber-Osguthorpe and Hagler[37] (Biosym software *INSIGHT II* and *DISCOVER*). The dynamics were run for 50 ps (variable temperature) or 300 ps (constant temperature). The trajectory was sampled by minimising and storing the structure every picosecond.

Acknowledgements

This work was supported by grants from Hoechst Marion Roussel (Romainville Research, Medicinal Chemistry). We thank James McCabe (Centre for Technical Languages, Université René Descartes-Paris V) for his critical reading of this manuscript.

References

1 J. R. Menninger, *J. Basic Clin. Physiol. Pharmacol.*, 1995, **6**, 229.
2 G. Bertho, J. Gharbi-Benarous, P. Ladam, M. Delaforge and J. P. Girault, *Bioorg. Med. Chem.*, 1998, **6**, 209.
3 R. C. Goldman, S. W. Fesik and C. C. Doran, *Antimicrob. Agents Chemother.*, 1990, **34**, 426.
4 R. Fernandez-Munoz and D. Vazquez, *J. Antibiot.*, 1973, **26**, 107.
5 S. Pestka, *Antimicrob. Agents Chemother.*, 1974, **6**, 474.
6 J. Barber, J. I. Gyi and D. A. Pye, *J. Chem. Soc.*, *Chem. Commun.*, 1991, 1249.
7 A. Awan, R. J. Brennan, A. C. Regan and J. Barber, *J. Chem. Soc.*, *Chem. Commun.*, 1995, **16**, 1653.
8 B. W. Dubois and A. S. Evers, *Biochemistry*, 1992, **31**, 7069.
9 Y. Fraenkel, G. Navon, A. Aronheim and J. M. Gershoni, *Biochemistry*, 1990, **29**, 2617.
10 J. J. Fischer and O. Jardetzky, *J. Am. Chem. Soc.*, 1965, **87**, 3237.
11 G. Bertho, J. Gharbi-Benarous, M. Delaforge, C. Lang, A. Parent and J. P. Girault, *J. Med. Chem.*, 1998, **41**, 3373.
12 J. Gharbi-Benarous, N. Evrard-Todeschi, P. Ladam, G. Bertho, M. Delaforge and J. P. Girault, *J. Chem. Soc.*, *Perkin Trans. 2*, 1999, 529.
13 G. Bertho, P. Ladam, J. Gharbi-Benarous, M. Delaforge and J. P. Girault, *Int. J. Biol. Macromol.*, 1998, **22**, 103.
14 N. Evrard-Todeschi, J. Gharbi-Benarous, C. Gaillet, L. Verdier, G. Bertho, C. Lang, A. Parent and J. P. Girault, *Bioorg. Med. Chem.*, 2000, 1579.
15 C. Agouridas, A. Denis, J. M. Auger, Y. Benedetti, A. Bonnefoy, F. Bretin, J. F. Chantot, A. Dussarat, C. Fromentin, S. Goin D'Ambrières, S. Lachaud, P. Laurin, O. Le Martret, V. Loyau and N. Tessot, *J. Med. Chem.*, 1998, **41**, 4080.
16 A. Denis, C. Agouridas, J. M. Auger, Y. Benedetti, A. Bonnefoy, F. Bretin, J. F. Chantot, A. Dussarat, C. Fromentin, S. Goin D'Ambrières, S. Lachaud, P. Laurin, O. Le Martret, V. Loyau, N. Tessot, J. M. Pejac and S. Perron, *Bioorg. Med. Chem. Lett.*, 1999, **9**, 3075.
17 L. Verdier, G. Bertho, J. Gharbi-Benarous and J.-P. Girault, *Bioorg. Med. Chem.*, 2000, **8**, 1225.
18 R. A. Dwek, *Nuclear Magnetic Resonance in Biochemistry: Applications to Enzyme Systems*, Clarendon Press, Oxford, 1973.
19 F. Ni, *Prog. Nucl. Magn. Reson. Spectrosc.*, 1994, **26**, 517.
20 R. E. London, *J. Magn. Reson.*, *Ser. A*, 1993, **104**, 190.
21 J. Feeney, J. G. Batchelor, J. P. Albrand and G. C. K. Roberts, *J. Magn. Reson*., 1979, **33**, 519.
22 A. Lanir and G. Navon, *Biochemistry*, 1971, **10**, 1024.
23 T. R. Tritton, *Arch. Biochem. Biophys.*, 1979, **197**, 10.
24 A. L. Barry, P. C. Fuchs and S. D. Brown, *Antimicrob. Agents Chemother.*, 1998, **42**, 945.
25 G. A. Pankuch, M. A. Visalli, M. R. Jacobs and P. C. Appelbaum, *Antimicrob. Agents Chemother.*, 1998, **42**, 624.
26 S. Panagea, J. D. Perry and F. K. Gould, *J. Antimicrob. Chemother.*, 1999, **44**, 577.
27 J. I. Gyi, R. J. Brennan, D. A. Pye and J. Barber, *J. Chem. Soc.*, *Chem. Commun.*, 1991, 1471.
28 R. J. Brennan, A. Awan, J. Barber, E. Hunt, K. L. Kennedy and S. Sadegholnejat, *J. Chem. Soc.*, *Chem. Commun.*, 1994, 1615.
29 J. R. Everett, I. K. Hatton and J. W. Tyler, *Magn. Reson. Chem.*, 1990, **28**, 114.
30 J. Gharbi-Benarous, P. Ladam, M. Delaforge and J. P. Girault, *J. Chem. Soc.*, *Perkin Trans. 2*, 1993, 2303.
31 B. Weisblum, *Antimicrob. Agents Chemother.*, 1995, **39**, 577.
32 M. P. Fournet, J. Barre, R. Zini, L. Deforges, J. Duval and J. P. Tillement, *J. Pharm. Pharmacol.*, 1987, **39**, 319.
33 P. Jelenc, *Anal. Biochem.*, 1980, **105**, 369.
34 M. Tsuchiya, K. Suzukake, M. Hori, T. Sawa and H. Umejawa, *J. Antibiot.*, 1981, **24**, 305.
35 C. L. Swenden and W. Johnson, *Infect. Immun.*, 1976, **14**, 345.
36 D. G. Davis, M. E. Perlman and R. E. London, *J. Magn. Reson.*, *Ser. B*, 1994, **104**, 266.
37 P. Dauber-Osguthorpe, V. A. Roberts, D. J. Osguthorpe, J. Wolff, M. Genest and A. T. Hagler, *Proteins: Struct. Funct. Genet.*, 1988, **4**, 31.